Scalar Beltramization in turbulent flows

Wouter J.T. Bos[1], Robert Rubinstein[2] and Le Fang[1]
[1] *LMFA, CNRS, Ecole Centrale de Lyon - Université de Lyon, Ecully, France and*
[2] *Newport News, VA, USA*

We show that in turbulent scalar mixing the advection is strongly suppressed with respect to its Gaussian estimate. This effect is particularly important in the small scales. Results are given for different Schmidt numbers, illustrating the persistency and universality of the phenomenon. The link with the generation of passive scalar fronts is discussed and it is argued that scalar fronts are the consequence of the underlying suppression of nonlinearity observed in a wide class of flows for which the dynamics are governed by quadratic nonlinearities or pseudo-nonlinearities.

PACS numbers: 47.27.Ak, 47.27.eb, 47.51.+a

The advection of a blob of scalar in a fluid in movement is governed by a linear partial derivative equation. Despite the apparent simplicity of the problem, the stretching and folding of the scalar blob will generally result in a complicated, multi-scale pattern, even in the case in which the flow-field is predictable. In the case of simple flow patterns, some characteristics of the mixing process can be understood on a deterministic level [1]. In the case in which the flow is stochastic, the scalar field is not easily amenable to such an approach and a statistical description is needed. The statistical approach will be adopted in the present letter to explain a typical feature observed in independent realizations of a scalar mixed by a turbulent, or random multi-scale flow: the persistence of small scale gradients, or fronts. An interesting feature of scalar mixing is that fronts are even generated when the advecting velocity field is structureless [2, 3]. This suggested that the problem of small scale intermittency could be studied by considering the scalar advection-diffusion equation in the hope to learn about the more complicated case of Navier-Stokes turbulence (see *e.g.* reference [4]). In reference [2, 3] a phenomenological explanation of the generation of fronts was proposed, based on the convergence of fluid parcels. In the present letter we do not propose another mechanism of front-generation but we show that the mechanism proposed in references [2, 3] can be seen as a consequence of a more general phenomenon called depletion of nonlinearity of which the discovery can be attributed to Kraichnan and Panda [5].

In turbulent flows, velocity and vorticity have a tendency to align in the small scales, leading to local helicity fluctuations. This alignment, called *Beltramization*, was suggested by Levich and Tsinober [6] to be dynamically important and its existence was first shown in simulations by Pelz *et al.* [7]. The alignment results in a weakening of the nonlinear term which can be readily seen from the Navier-Stokes equations. The Fourier tranformed Navier-Stokes equations can be written as

$$\left[\partial_t + \nu k^2\right] \hat{u}_i(\boldsymbol{k}) = P_{ij}(\boldsymbol{k})\hat{\lambda}_j(\boldsymbol{k}) + \hat{f}_i(\boldsymbol{k}) \qquad (1)$$

in which ν is the kinematic viscosity, $\boldsymbol{\lambda} = \boldsymbol{\omega}(\boldsymbol{x}) \times \boldsymbol{u}(\boldsymbol{x})$, with $\boldsymbol{\omega}$ the vorticity, $P_{ij}(\boldsymbol{k}) = \delta_{ij} - k_i k_j k^{-2}$ is the Riesz projector and $\boldsymbol{f}(\boldsymbol{k})$ an external forcing. All quantities in which the time argument is omitted are implicitly assumed to be evaluated at time t.

Clearly, if the Lamb-vector $\boldsymbol{\lambda}(\boldsymbol{x})$ is equal to zero, the nonlinearity vanishes. A later study by Rogers and Moin [8], showed, in contrast to [7], that in a number of different turbulent flow geometries, this mechanism was not clearly observed. This observation was confirmed by the analysis of Kraichnan and Panda [5], who investigated the suppression of nonlinearity by comparing the mean-square nonlinearity of Navier-Stokes turbulence with its value in a Gaussian field with the same kinetic energy wavenumber spectrum. In their study it was shown that Beltramization is not strong enough to account for the suppression of nonlinearity observed in simulations of Navier-Stokes turbulence. A certain alignment of the Lamb-vector $\boldsymbol{\lambda}$ with the wave-vector $\boldsymbol{k}$ is needed to explain the observed reduction of nonlinearity. This observation combined with the fact that they observed the same effect in the statistics of Betchov model equations, led Kraichnan and Panda to the suggestion that the effect was not caused by topological constraints but that it was a phenomenon observed in a wider class of flows containing quadratic nonlinearities.

In the present work we will show that this effect can be transposed to the advection of a passive scalar $\theta(\boldsymbol{x}, t)$. Furthermore, it will be argued that this effect leads to the persistence of strong gradients or fronts observed in the fine scales of the scalar field.

The equation for the advection of a passive scalar is,

$$\left[\partial_t + \alpha k^2\right] \hat{\theta}(\boldsymbol{k}) = -ik_i\hat{\gamma}_i(\boldsymbol{k}) + \hat{f}_\theta(\boldsymbol{k}) \qquad (2)$$

with $\gamma_i = u_i(\boldsymbol{x})\theta(\boldsymbol{x})$ and $\hat{f}_\theta(\boldsymbol{k})$ a scalar source term, that we will assume confined to the large scales. The diffusivity of the scalar is denoted by α. Strictly speaking the advection term is not a quadratic nonlinearity, but as we will see, an analogous effect is observed for the advection as is for the nonlinearity of the Navier-Stokes equation. We will call the advection term in this context a pseudo-nonlinearity.

Let us compare the structure of the nonlinear term of the Navier-Stokes equation (1) and the advection term in

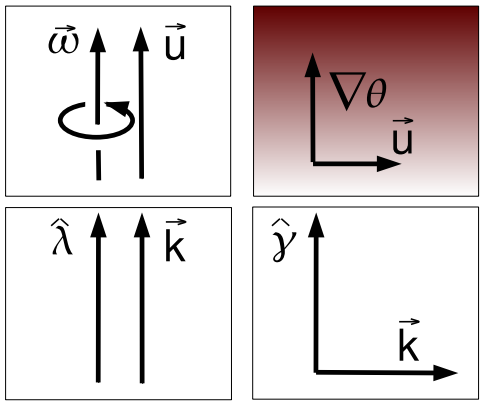

FIG. 1: Left, top: velocity Beltramization; bottom: depletion of nonlinearity through alignment of the Lamb-vector and the wavevector. Right: scalar Beltramization in physical and Fourier space.

equation (2). There are two non-trivial ways to reduce the nonlinearity in (1). Firstly the alignment of velocity and vorticity so that $\boldsymbol{\lambda} = 0$, secondly the alignment of the Lamb-vector with the wavevector. These two possibilities are illustrated in Figure 1 (left). Both possibilities can, and do, contribute to the depletion of nonlinearity in turbulent flows. For the passive scalar the equivalent of the first possibility would be the vanishing of the vector $\boldsymbol{\gamma} \equiv \theta \boldsymbol{u}$. We do not consider this trivial possibility in which either the velocity or the scalar is zero. The only non-trivial possibility to reduce the advection term is the tendency of the vector $\boldsymbol{\gamma}$ to be perpendicular to the wavevector. Since

$$i\boldsymbol{k} \cdot \hat{\boldsymbol{\gamma}} = \widehat{\nabla \cdot \boldsymbol{\gamma}} = \widehat{\boldsymbol{u} \cdot \nabla \theta}, \tag{3}$$

this corresponds to the case in which the velocity is perpendicular to the scalar gradient, as illustrated in Figure 1 (right). In analogy to the mechanism of Beltramization, which is one of the possible mechanisms to reduce nonlinearity in a turbulent velocity field, we will call the geometry in which the scalar gradient is perpendicular to the velocity field *scalar Beltramization*. We stress here that for the velocity field it is not the only mechanism which suppresses nonlinearity (the other mechanism being the alignment of the Lamb-vector with the wavevector), however, scalar Beltramization corresponds to the only non-trivial geometry which reduces the strength of the advection. The goal of the present work is to investigate whether a reduction of advection (or scalar flux variance) is indeed observed in turbulent mixing.

To measure to what extent the turbulent advection is suppressed in a turbulent flow, we will consider the mean-square of the advection. The quantity we focus on is the spectrum of the advection term, normalized so that the integral is equal to the scalar flux variance,

$$\int w_\theta(k) dk = \overline{[\boldsymbol{u}(\boldsymbol{x}) \cdot \nabla \theta(\boldsymbol{x})]^2}. \tag{4}$$

In addition to giving the strength of the advection, the wavenumber spectrum also gives insight on its scale dependence. The spectrum $w_\theta(k)$ is then given by

$$w_\theta(k) = 4\pi k^2 k_i k_j \overline{\hat{\gamma}_i(\boldsymbol{k}) \hat{\gamma}_j(-\boldsymbol{k})} \tag{5}$$

We will compare the spectrum to its Gaussian estimate $w_\theta^G(k)$, in which we will consider a scalar field $\zeta_\theta(\boldsymbol{x}, t)$, with the same scalar variance spectrum as the true field, in other words,

$$\overline{\zeta_\theta(\boldsymbol{k}) \zeta_\theta^*(\boldsymbol{k})} \equiv \overline{\theta(\boldsymbol{k}) \theta^*(\boldsymbol{k})} = (2\pi k^2)^{-1} E_\theta(k) \tag{6}$$

with $E_\theta(k)$ the scalar variance spectrum. In the following we will in particular investigate the ratio $w_\theta(k)/w_\theta^G(k)$. This ratio can be interpreted as a measure of non-Gaussianity of the strength of the advection as a function of lengthscale. If this quantity is equal to one, the scalar advection is as strong as it would be if the scalar field were Gaussian.

In direct numerical simulations $w_\theta(k)$ can be determined directly using expression (5). The Gaussian estimate $w_\theta^G(k)$ is then obtained by replacing the vector-field $\theta(\boldsymbol{x}, t)$ by $\zeta_\theta(\boldsymbol{x}, t)$. This field can be readily obtained by randomizing the phases of the Fourier-coeffients $\hat{\theta}(\boldsymbol{k}, t)$. This will yield a field with Gaussian statistics and leaves unchanged the wavenumber spectrum since the values of the amplitudes of the Fourier-coeffients are not changed. This procedure was carried out using data of high resolution (1024^3 gridpoint) pseudospectral direct numerical simulations (DNS) of an isotropic scalar advected by isotropic turbulence. Details on the data and the simulation can be found in [9], low resolution observations of the depletion of advection are reported in [10].

A disadvantage of DNS is that its resolution is limited to moderately high Reynolds and Péclet numbers. Furthermore, statistics of the large scales are at these Reynolds numbers poorly converged since the computation can only be carried out for a limited number of eddy turn-over times and the large scales are resolved by a relatively small number of Fourier modes. To study the statistics of high Reynolds number turbulence, two-point closures are a useful tool. Their geometrical discretization allows to attain very high Reynolds numbers (*e.g.* [11]), and since the method considers ensemble-averages, no averaging is needed to obtain converged statistics. Several textbooks on the subject [12–14] give details on these methods and report on their capabilities to contribute to the understanding of turbulence at asymptotically high Reynolds number.

The closure expression for $w_\theta(k)$ will now be obtained, using the Direct Interaction Approximation (DIA)[15], which can be considered the cornerstone of the analytical theory of turbulence. In order not to digress unnecessarily from the physical ideas, only a short outline is given of the derivation of the closure expression. Two procedures are outlined in [16] to obtain DIA expressions for higher-order quantities. One of these is based on the use of generalized Langevin models [17]. The other method is

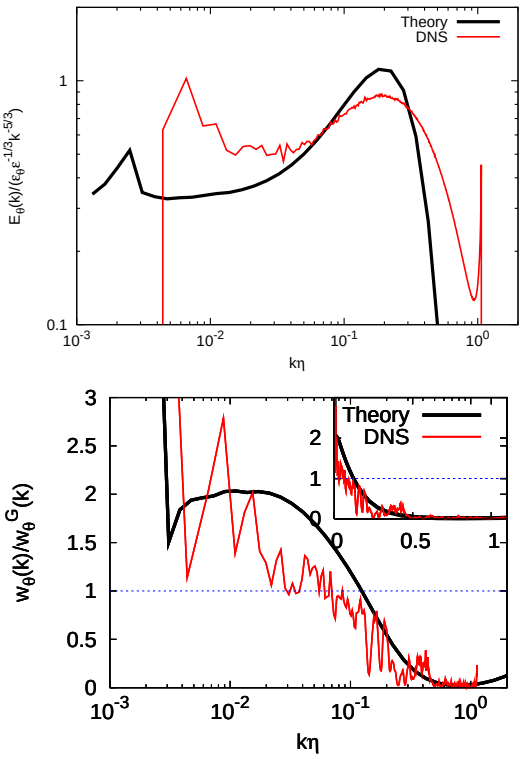

FIG. 2: DNS and theoretical results. Top: compensated scalar spectra in isotropic turbulence at a Taylor-scale Reynolds number of 427 and $\mathcal{S}c = 1$. Bottom: comparison of the spectrum of the mean square advection term of the scalar equation in isotropic turbulence to its Gaussian value. In the inset the same results are plotted in linear representation.

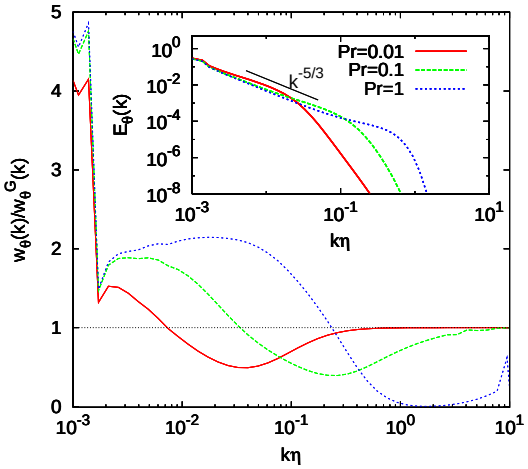

FIG. 3: Comparison of the spectrum of the mean square advection term of the scalar equation in isotropic turbulence to its Gaussian value at a Taylor-scale Reynolds number of 1000 and $\mathcal{S}c = 0.01, 0.1, 1$. Inset: scalar variance spectra.

by means of a second-order DIA perturbation approach. Both methods lead to the same expression,

$$w_\theta(k) = w_\theta^G(k) + w_\theta^C(k) \tag{7}$$

with

$$w_\theta^G(k) = k^3 \int_\Delta (1-z^2) E(p) E_\theta(q) \frac{dp}{p}\frac{dq}{q} \tag{8}$$

and

$$w_\theta^C(k) = \frac{1}{2}\iint_\Delta \iint_{\Delta'} (1-z^2) kq^2 E(p) (1-z'^2) kq'^2 E(p') \times \left[\left(\Xi_{kpqp'q'} + \Xi_{kp'q'pq}\right) E_\theta(k) - 2\Xi_{kpqp'q'} kq^{-1} E_\theta(q)\right] \times \frac{dp'}{p'}\frac{dq'}{q'}\frac{dp}{p}\frac{dq}{q} \tag{9}$$

where Δ indicates that the integration domain is confined to the wavevectors $\boldsymbol{k}, \boldsymbol{p}, \boldsymbol{q}$ which can form a triangle and z is the cosine of the angle between $\boldsymbol{k}$ and $\boldsymbol{p}$. The manipulations needed to obtain (9) are standard in DIA and for details we refer to [12]. Technical details on and theoretical considerations about the derivation of these expressions will be published elsewhere. In expression (9), the time-scale Ξ can be obtained by assuming an exponential time-dependence of all two-time quantities and a relation between the energy spectra and the response functions, given by the flucuation-dissipation theorem. In the long-time limit the time-scale will then be given by

$$\Xi_{kpqp'q'} = \frac{1}{\eta_k^\theta + \eta_{p'} + \eta_{q'}^\theta} \frac{1}{\eta_p + \eta_q^\theta + \eta_{p'} + \eta_{q'}^\theta} \tag{10}$$

in which η_k and η_k^θ are turbulent time-scales related to the velocity and scalar correlations respectively. These time-scales can be chosen as in standard EDQNM type closures. In the present work we will use the self-consistent closure presented in [19], in which η_k is determined without the introduction of a model constant. An analytical check of the above equations is that the cumulant contributions should vanish in the case of thermal equilibrium, in which the statistics are supposed to be Gaussian. Indeed, using the fluctuation-dissipation theorem which is exact in this case, one can show that (9) vanishes when the scalar field is in equipartition, independent of the choice of the time-scale. Note that in this derivation we considered mirror-symmetric isotropic turbulence. The influence of helicity constitutes an interesting perspective.

In Figure 2 we compare the results of DNS and closure. In the top figure we show the spectrum of the scalar variance in compensated form. The wavenumber of the DNS results is normalized by the Kolmogorov scale, which is equal to the Batchelor scale for unity Schmidt number. The wavenumber of the closure results is normalized by the wavenumber at which the compensated DNS spectrum peaks. It is well-known that closures of the Lagrangian DIA [20] family underestimate the inertial range

level of the scalar spectrum. This is also the case here, but we will not focus further on this issue. On the bottom figure we show the comparison of $w_\theta(k)/w_\theta^G(k)$. Even though the quantitative agreement is only approximate, both curves show an important suppression of advection in the small scales. It is possible that this agreement will improve if the DNS results for $E(k)$ and $E_\theta(k)$ are used in the closure expression for $w_\theta(k)/w_\theta^G(k)$, but that will be left for future work. It is at this point enough to say that the effect we investigate is clearly observed both in DNS and closure. Since the spectrum $w_\theta(k)$ is an increasing function of the wavenumber in the inertial range, it is the large wavenumber end of the spectrum which determines the integral value of the mean-square advection. It is therefore not the small wavenumbers, at which a super-Gaussian value is observed, which determine the integral value.

It is interesting to know how this *scalar-Beltramization*, depends on the relative location of the viscous and diffusive ranges, in other words, how it depends on the Schmidt or Prandtl number. To investigate this we vary the Schmidt number, defined as $\mathcal{S}c = \nu/\alpha$ by a factor 100, from 0.01 to 1. We do this at a Reynolds number of $R_\lambda = 1000$. In Figure 3 we show the closure results. It is observed that the region in which the scalar Beltramization takes place moves with the diffusive scale of the passive scalar. This shows that the lengthscales at which the depletion of advection is observed, are not determined by the viscous subrange of the kinetic energy distribution, but are determined by the scalar diffusive scale. The scalar Beltramization is therefore an intricate mechanism, involving both the effects of nonlinear mode coupling and diffusion.

We can conclude that scalar Beltramization is observed in scalar mixing. Geometricallly this corresponds to the case in which the velocity is perpendicular to the scalar gradients as shown in Figure 1 (right). This particular geometry will favour the generation of fronts (a phenomenon we can also call frontogenesis), since the scalar gradients will not be mixed by a perpendicular velocity. Fronts of passive scalar are indeed observed in turbulent mixing, see for example reference [9], for the case of isotropic turbulence, advecting an isotropic scalar. In particular, this example shows that no external effects introducing anisotropy or inhomogeneity are needed to explain the typical small scale behavior of a scalar field. Only the intrinsic tendency towards a state with reduced nonlinearity [5] is needed to create the characteristic fine scale structure observed in turbulent mixing. Another way to phrase this is that, if the velocity and scalar would not only be uncorrelated, as is the case in isotropic turbulent mixing, but also independent, which is what the Gaussian estimate assumes, there could not possibly be any scalar fronts. Fronts are therefore a signature of the statistical dependence of θ and $\boldsymbol{u}$, which is observed in the present study.

We anticipate that, according to our analysis, the effect should also be observed if the advecting velocity field is Gaussian. Indeed, in our analysis the only non-Gaussian contributions to the mean-square advection stem from the perturbation of the passive scalar fluctuation in (5). This is in agreement with observations of the creation of scalar fronts in advection by a Gaussian velocity field [2, 21].

It might seem surprising that if the depression of advection is linked to the marked fronts observed in the fine scales, it could be captured by statistical closures. Indeed it is often mistakenly assumed that these approaches can not predict anything on structure related issues since all phase-information is averaged out. The apparent paradox stems from the fact that structures are a dynamical consequence of the underlying equations and the statistical theories are derived from these equations. It is therefore not completely surprising that, if the assumptions used in deriving the closures are physically sound, the statistics observed from closures can be related to the structures observed in experiments and simulations

Acknowledgments. The authors are indebted to Toshiyuki Gotoh and the CINECA database for making the DNS data available.

[1] J. Ottino, *The kinematics of mixing: stretching, chaos and transport*, Cambridge University Press, 1989.
[2] M. Holzer and E. Siggia, Phys. Fluids A **6**, 1820 (1994).
[3] B. Shraiman and E. Siggia, Nature **405**, 639 (2000).
[4] A. Celani, A. Lanotte, A. Mazzino, and M. Vergassola, Phys. Fluids **13**, 1768 (2001).
[5] R. Kraichnan and R. Panda, Phys. Fluids **31**, 2395 (1988).
[6] E. Levich and A. Tsinober, Phys. Lett. **93A**, 293 (1983).
[7] R. Pelz, V. Yakhot, S. Orszag, L. Shtilman, and E. Levich, Phys. Rev. Lett. **54**, 2505 (1985).
[8] M. M. Rogers and P. Moin, Phys. Fluids **30**, 2662–2671 (1987).
[9] T. Watanabe and T. Gotoh, New J. Phys. **6**, 40 (2004).
[10] J. Herring and O. Métais, J. Fluid Mech, **235**, 103 (1992).
[11] W. Bos, H. Touil, and J.-P. Bertoglio, Phys. Fluids **17**, 125108 (2005).
[12] D. Leslie, *Developments in the theory of turbulence*, Oxford University Press, 1973.
[13] M. Lesieur, *Turbulence in fluids*, Kluwer Dordrecht, 1990.
[14] P. Sagaut and C. Cambon, *Homogeneous Turbulence Dynamics*, Cambridge University Press, 2008.
[15] R. Kraichnan, J. Fluid Mech. **5**, 497–543 (1959).
[16] H. Chen, J. Herring, R. Kerr, and R. Kraichnan, Phys. Fluids A **1**, 1844 (1989).
[17] R. Kraichnan, J. Fluid Mech. **41**, 189 (1970).
[18] G. R. Newman and J. Herring, J. Fluid Mech, **94**, 163 (1979).
[19] W. Bos and J.-P. Bertoglio, Phys. Fluids **18**, 031706 (2006).
[20] R. Kraichnan, Phys. Fluids **8**, 575 (1965).

[21] S. Chen and R. H. Kraichnan, Phys. Fluids **10**, 2867 (1998).